Lecture #23: Collisionless Magnetic Reconnection

I. Key Questions about the Physics of Magnetic Reconnection

A. Key Questions

1. What triggers the sudden onset of magnetic reconnection?
   e.g., Solar Flares: Slow evolution for weeks or months, followed by sudden release of energy in 20 minutes.

2. What is the effective rate of magnetic reconnection?

3. Partitioning of Released Magnetic Energy:

   a. How is released magnetic energy split between ions & electrons?

   b. What is the division among kinetic energy of bulk outflows, plasma heating of ions and electrons, and acceleration of a small fraction of particles to high energy

II. Fast Magnetic Reconnection

A. Reconnection Timescales

1. Both the Sweet-Parker model and the linear tearing instability are examples of slow magnetic reconnection
   a. Sweet Parker $\tau_r \sim S^{\frac{1}{2}} \tau_A$
   b. Tearing Instability $\tau_{ti} \sim \frac{1}{\gamma} \sim S^{\frac{3}{5}} \tau_A$

2. Example: X-class Solar flare

a. Parameters:

Quantity	Value
T_{obs}	100 s
B_0	0.01 T
n_0	$10^{16}\,m^{-3}$
L	$10^7\,m$
Flux Tube Area $\propto L^2$	$10^{14}\,m^2$
T_i	$10^6\,K$
T_e	$10^6\,K$

b. Computed Quantities

Quantity	Value
V_A	$2\times10^6\ \frac{m}{s}$
Plasma Parameter, Λ	1.4×10^7
Coulomb log, $\ln\Lambda$	16
ν_{ei}	$1.6\times10^3\ s^{-1}$
η	$5.6\times10^{-3}\ \frac{kg\,m^3}{C^2 s}$
S	5×10^{12}

SI units:

i) $\Lambda = \frac{4\pi}{3}\lambda_D^3 n_0 = \frac{4\pi}{3}\left(\frac{\epsilon_0 k T_e}{e^2 n_0}\right)^{3/2} n_0$

$$\boxed{\Lambda = \frac{4\pi(\epsilon_0 k T_e)^{3/2}}{3e^3 n_0^{1/2}}}$$

ii) $$\boxed{\nu_{ei} = \left(\frac{e^4}{2^{5/2}\pi\,\epsilon_0^2 m_e^{1/2}}\right)\frac{n_0}{(kT_e)^{3/2}}\ln\Lambda}$$

iii) $$\boxed{\eta = \frac{m_e \nu_{ei}}{e^2 n_0}}$$

iv) $$\boxed{S \equiv \frac{\mu_0 V_A L}{\eta}}$$

c. Timescales:

T_{obs}	~100 s
Alfven Time, $\tau_A \sim \frac{L}{V_A}$	5 s
S-P Rxn, $\tau_r \sim S^{1/2}\tau_A$	10^7 s ~ 0.3 years
Resistive Diff, $\tau_R \sim \frac{\mu_0 L^2}{\eta}$	2×10^{13} s ~ 7×10^5 years

$$\boxed{\text{Observed time corresponds to } U_{in} \sim 0.1\,V_A}$$

B. <u>Plasmoid Instability</u> - Faster MHD Reconnection

1. Recall from the Sweet-Parker model, $\frac{\delta}{\Delta} \sim S^{-\frac{1}{2}}$

a. As η decreases, & thus S increases, the current sheet becomes increasingly thin.

b. This dependence of δ on S (assumed independence in simple Sweet-Parker model) leads to an instability of the thinning current sheet

$\Rightarrow$ $\boxed{\text{Plasmoid instability}}$ Loureiro, Schekochihin, & Cowley, PoP 14:100703 (2007)

2. This very rapidly growing tearing instability

a. Breaks up current layer, producing plasmoids that effectively increase the reconnection rate.

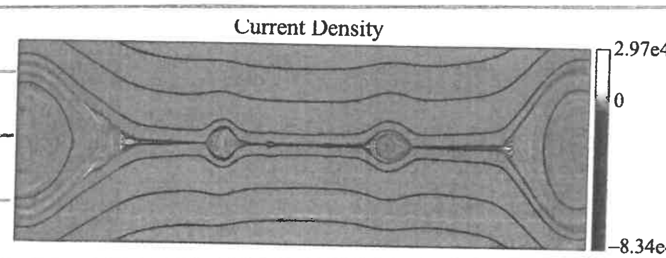

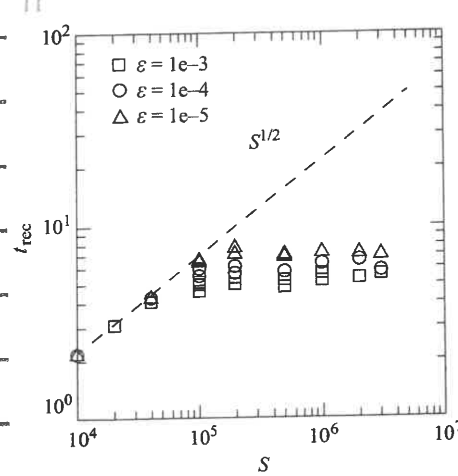

b. Above a critical Lundquist number $S_c \sim 10^4$, the reconnection rate becomes nearly independent of S.

$\Rightarrow$ $\boxed{\text{Leads to regime of fast reconnection in resistive MHD}}$

Ref: Huang & Bhattacharjee PoP 17:062104 (2010).

III. Collisionless Magnetic Reconnection

A. Kinetic Physics of Magnetic Reconnection

1. MHD approximation assumes strongly collisional conditions, so ion and electron fluid move together.

2. But, in many plasmas — such as space and astrophysical plasmas, or fusion plasmas in the lab — the mean free path for collisions ($\lambda_{mfp} \gtrsim \delta$) is larger than the current sheet width. $\Rightarrow$ $\boxed{\text{weakly collisional}}$

3. Furthermore, an MHD description cannot explain
   a. Partitioning of energy between ions and electrons
   b. Acceleration of small fraction of particles to high energy.

   $\Rightarrow$ $\boxed{\text{Requires kinetic model of the plasma physics}}$

4. Changes from Sweet-Parker Model:
   a. In Sweet-Parker, $\Delta \sim L$ (macroscopic length) and δ is a function of resistivity.
   b. Thus $U_{in} \sim \frac{\delta}{\Delta} V_A$ $\rightarrow$ inflow limited by geometry (L) & resistivity.
   c. In a kinetic plasma, where $\eta \rightarrow 0$, what physics controls δ and Δ?

   $\Rightarrow$ $\frac{\delta}{\Delta}$ will still control reconnection rate.

B. Length Scales of Collisionless Magnetic Reconnection

1. Generalized Ohm's Law:

$$\underset{\sim}{E} + \underset{\sim}{u} \times \underset{\sim}{B} = \eta \underset{\sim}{j} + \underbrace{\frac{1}{en} \underset{\sim}{j} \times \underset{\sim}{B}}_{\text{Hall term}} - \underbrace{\frac{1}{en} \nabla \cdot \underset{\approx}{P}_e}_{\text{electron pressure tensor}} + \underbrace{\frac{m_e}{e^2 n}\left[\frac{\partial \underset{\sim}{j}}{\partial t} + \nabla \cdot (\underset{\sim}{j}\underset{\sim}{u} + \underset{\sim}{u}\underset{\sim}{j})\right]}_{\text{electron inertia}}$$

Take $\eta \to 0$ in weakly collisional plasma

$\delta \lesssim \underbrace{d_i}_{\text{ion inertial length}} = \frac{c}{\omega_{pi}}$

$\delta \lesssim \underbrace{\rho_s = \frac{c_s}{\Omega_i}}$ ion sound Larmor radius, where $c_s = \left(\frac{T_e}{m_i}\right)^{\frac{1}{2}}$ where $T_e \gg T_i$

$\delta \lesssim d_e = \frac{c}{\underbrace{\omega_{pe}}}$ electron skin depth

2. From linear wave dispersion relation (Vlasov-Maxwell), waves become dispersive (phase and group velocities dependence on $\underset{\sim}{k}$) for

$$\boxed{k d_i > 1 \quad \text{or} \quad k\rho_s > 1}$$

a. At scales $kd_i > 1$ or $k\rho_s > 1$, the
$\boxed{\text{ion motion decouples from the electron motion.}}$

3. What breaks frozen-in condition (which term in Ohm's law)?

a. Very near X-line, local velocity is small ($\underset{\sim}{j} \to 0$, $\underset{\sim}{u} \to 0$).
$\Rightarrow$ only the nongyrotropic electron pressure
$\frac{1}{ne} \nabla \cdot \underset{\approx}{P}_e$ balances reconnection electric field
(Vasyliunas, 1975)

C. Reconnection with Zero Guide Field ($b_g = 0$)

1. Consider again the Harris Sheet equilibrium

$$\underset{\sim}{B}_0 = B_{L0} \tanh\left(\frac{x}{a}\right) \hat{y} + B_{z0} \hat{z}$$

2. Define: Guide Field Ratio, b_g

$$\boxed{b_g \equiv \frac{B_{z0}}{B_{L0}}} \qquad \left(\frac{\text{out-of-plane } \underset{\sim}{B}}{\text{upstream in-plane } \underset{\sim}{B}_L}\right)$$

3. Relevant to Collisionless Magnetic Reconnection in Earth's Magnetotail

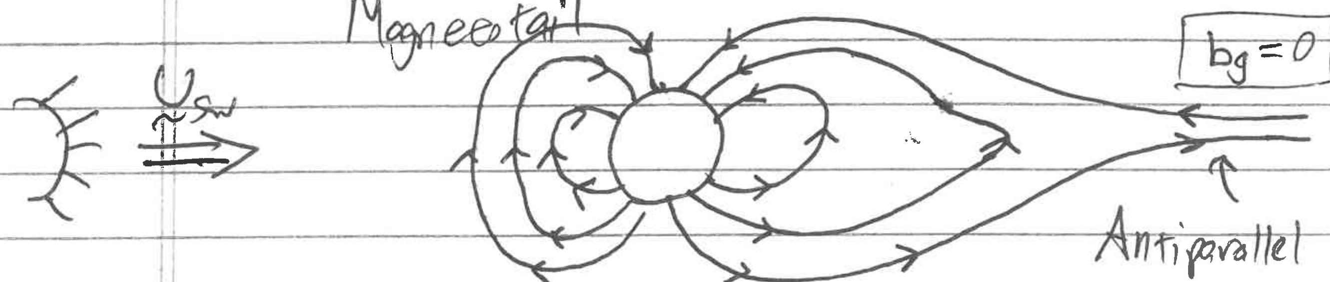

$\underset{\sim}{U}_{sw}$

$\boxed{b_g = 0}$

Antiparallel $\underset{\sim}{B}$ in magnetotail

$r \sim 10$ to $20\, R_E$

4. Ion & Electron Diffusion Regions

$\Rightarrow$ Multi-Scale Structure

Ion Diffusion Region (Ions decouple from magnetic field)

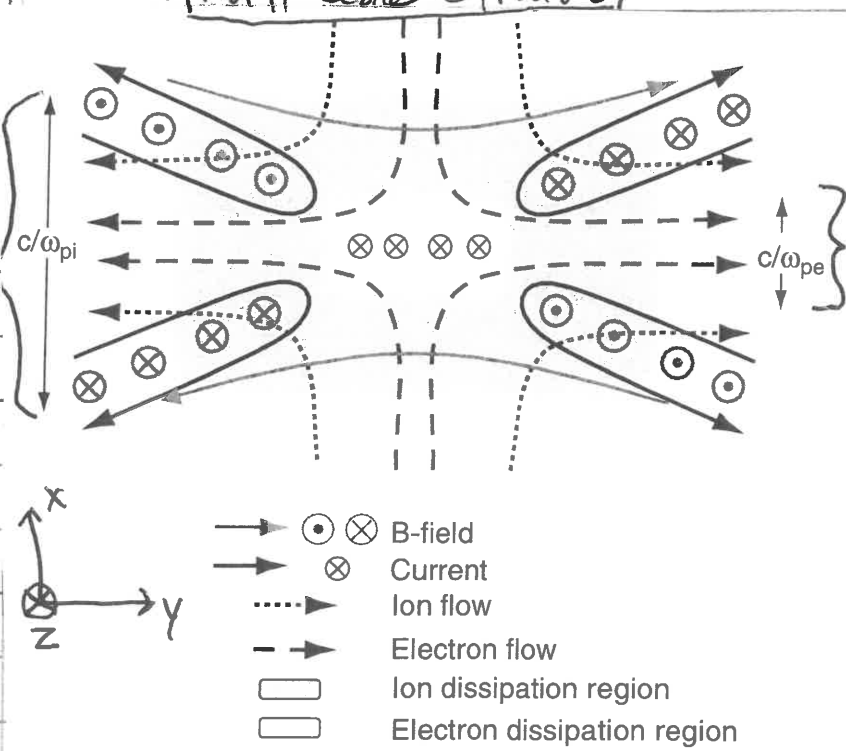

Electron Diffusion Region (electrons decouple from magnetic field)

Ref. ~~Birn & Priest, Reconnection of Magnetic Fields, Cambridge,~~ (2007)

5. Dynamics:

a. Upstream at $|x| > d_i$, ions & electrons flow together.

b. At $|x| < d_i$, ion motion decouples from electron & magnetic field flow, and ions are diverted to outflow.

c. For $d_e < |x| < d_i$, ions are demagnetized, but magnetic field is still frozen into electron flow.

d. At $|x| < d_e$, electrons cease to be frozen-in and they divert to the outflow

6. Outflow Speeds:

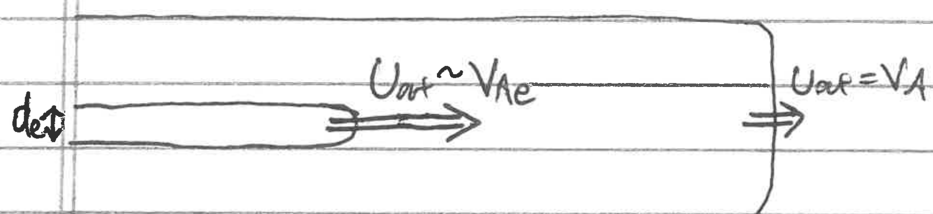

a. $$V_{Ae} = \frac{B}{\sqrt{\mu_0 n_e m_e}} = V_A \sqrt{\frac{m_i}{m_e}} \gg V_A = \frac{B}{\sqrt{\mu_0 n_i m_i}}$$ (where $n_i = n_e$)

b. Fast outflow from electron diffusion region $U_{out} = V_{Ae}$ slows down to $U_{out} = V_A$ at end of ion diffusion region.

7. Out-of-plane B_z:

a. Differential ion & electron flow within ion diffusion region leads to currents in perpendicular plane

b. Creates quadrupolar pattern of B_z

$\Rightarrow$ Signature of Whistler Wave Physics.

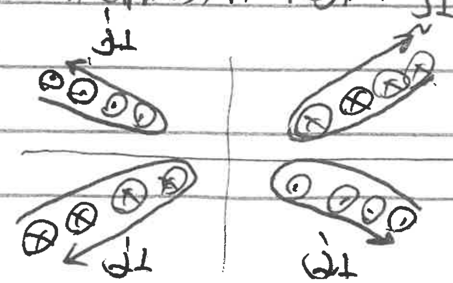

8. <u>Key Feature of Zero-Guide-Field Reconnection</u>

a. When Hall term is included in Ohm's Law, the diffusion region is localized in the (y) <u>outflow direction</u>,

So $\Delta \sim 10 d_i \ll L$

b. For Sweet-Parker $\Delta \sim L$

c. The ion diffusion region has $\delta \sim d_i$,

thus $\frac{\delta}{\Delta} \sim \frac{d_i}{10 d_i} \sim 0.1$, So $\boxed{U_{in} = \frac{\delta}{\Delta} V_A = 0.1 V_A}$

$\Rightarrow$ $\boxed{\text{Fast Reconnection}}$

d. <u>Dispersive nature of whistler waves</u> is responsible for this faster reconnection dynamics.

D. <u>Coupling to Whistler Waves for $b_g = 0$:</u>

1. Consider how linear plasma response, characterized by the linear wave physics, dictates the outflow velocity

2.

Effective B_0 for this "wave"

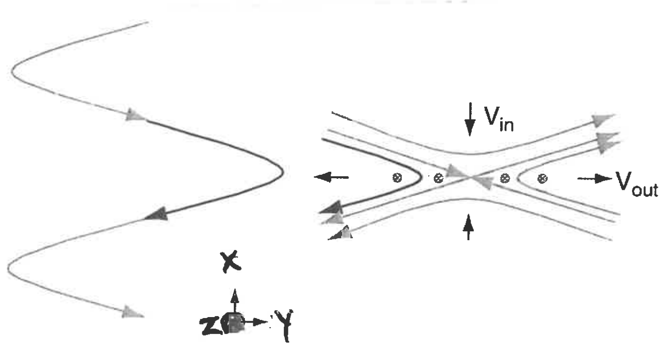

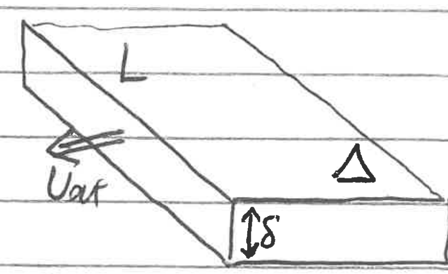

Particle flux in outflow

a. $\boxed{n U_{out} L \delta}$

III. D. (Continued)

3. For Resistive MHD (Sweet-Parker), Alfven wave governs outflow.

a. $\omega = k_{\parallel} v_A \Rightarrow \frac{\omega}{k_{\parallel}} = v_A$

b. $n U_{out} L \delta = n (v_A) L \delta \propto \delta \leftarrow$ If δ decreases, particle outflux decreases.

4. For whistler waves,

a. $$\frac{\omega}{\Omega_i} = \frac{m_i}{m_e} \left\{ \frac{k d_e \left[\frac{m_e}{m_i} + (k_{\parallel} d_e)^2 \right]^{\frac{1}{2}}}{1 + (k_{\parallel} d_e)^2} \right\}$$

b. Using $\frac{d_e}{d_i} = \sqrt{\frac{m_e}{m_i}}$ and $d_i = \frac{v_A}{\Omega_i}$, we can manipulate this eq

$$\boxed{\frac{\omega}{k v_A} = \frac{\left[1 + (k_{\parallel} d_i)^2 \right]^{\frac{1}{2}}}{1 + (k_{\parallel} d_e)^2}}$$ Whistler Wave Linear Dispersion Relation

5. In the $b_g = 0$ diffusion region, $d_e < \lambda_{\parallel} < d_i$

a. Thus, generally $k_{\parallel} d_i \sim \frac{d_i}{\lambda} \gg 1$

and $k_{\parallel} d_e \sim \frac{d_e}{\lambda} \ll 1$

b. For parallel propagation $k_{\parallel} \gg k_{\perp} \rightarrow k \sim k_{\parallel}$, and we obtain

$$\frac{\omega}{k_{\parallel} v_A} = \frac{\left[\cancelto{0}{1+} (k_{\parallel} d_i)^2 \right]^{\frac{1}{2}}}{1 + \cancelto{0}{(k_{\parallel} d_e)^2}} \simeq k_{\parallel} d_i$$

c. Phase velocity $\boxed{\frac{\omega}{k_{\parallel}} \sim (k_{\parallel} d_i) v_A}$

III. D. (Continued)

6. Ion out flux in whistler regime:

a. $n\, U_{out}\, L\delta \sim n(k_{\parallel} d_i v_A) L\delta$

b. But $k_{\parallel} \sim \frac{1}{\lambda_{\parallel}} \sim \frac{1}{\delta}$ ← current sheet thickness

c. So $n\left(\frac{d_i}{\cancel{\delta}} v_A\right) L \cancel{\delta} \sim n\, L\, d_i\, v_A$ ← Independent of current sheet thickness!

7. a. Since the outward flux of electrons from the dissipation region is independent of δ (thickness), the dynamics is independent of the mechanism that breaks the frozen-in condition.

b. Thus, rate of reconnection is independent of dominant non-ideal term in Ohm's Law!

8. GEM Reconnection Challenge
Ref: Birn, et al. JGR 106: 3715 (2001)

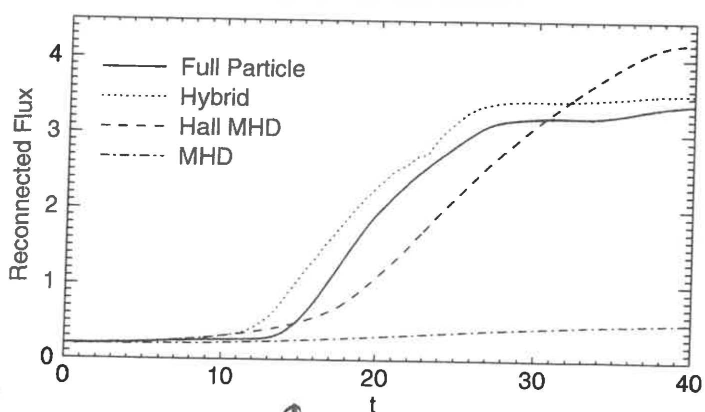

Harris Equilibrium, $b_g = 0$, $S \sim 200$

Different physics breaks magnetic field.

a. All models containing dispersive physics of whistler wave (Hall term) obtain fast reconnection rate.

b. Only MHD (no Hall term, only resistive) obtains slow, Sweet-Parker reconnection rate.

III. (Continued)

E. Reconnection with a Guide Field, $b_g \neq 0$

1. The introduction of a non-zero guide field B_{z0} ($b_g \neq 0$) substantially changes the structure of the reconnection diffusion region

2. The out-of-plane reconnection electric field E_z now has a component parallel to the total $\underset{\sim}{B} = \underset{\sim}{B}_{\perp 0} + B_{z0}\hat{z}$.

   a. Drives strong out-of-plane currents
   b. Parallel electron flow across x-line/current layer creates a quadrupolar density perturbation in electrons

3. When $b_g \neq 0$, reconnection dynamics couples to the physics of the Kinetic Alfven wave.

4. a. With non-zero magnetic field at the x-point when $b_g \neq 0$, current layer narrows to electron Larmor radius, $\delta \sim \rho_e$

   b. Enables non-gyrotropic $\underset{\sim}{P}_e$ at x-line to persist in breaking the magnetic field, even at $b_g \gg 1$.

   c. Also, ion diffusion region thickness scales as $\rho_i = \frac{v_{ti}}{\Omega_i}$

5. Ion & Electron Diffusion Regions $\boxed{\text{Multi-Scale Structure}}$

Ion Diffusion Region ρ_i

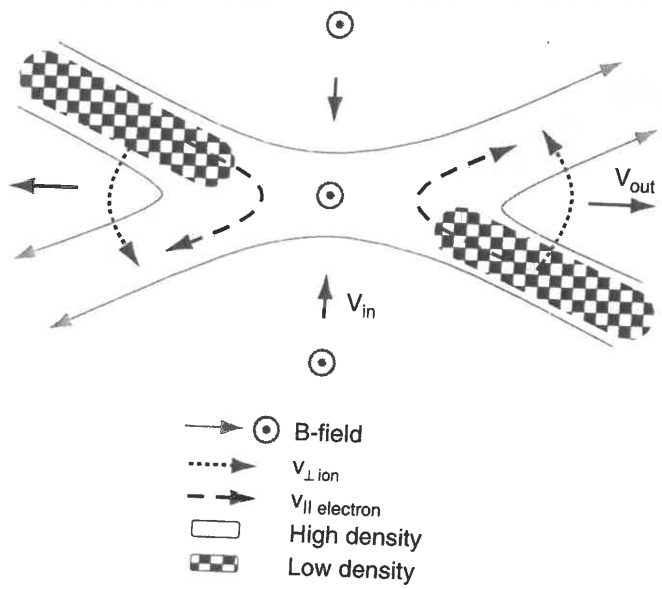

Electron Diffusion Region ρ_e

Ref: Birn & Priest (2007)

F. Coupling to Kinetic Alfven Waves for $b_y \neq 0$

1. Density asymmetry along separatrices is the signature of the Kinetic Alfven wave.

   a. Reconnection Electric field (out-of-plane) drives electron flow along $\underline{B}_{tot}$ across x-line/current layer

   b. Quadrupolar density perturbation results.

   c. Ions polarization drift across current layer to charge neutralize

2. Kinetic Alfven Waves:

   a. $$\boxed{\frac{\omega}{k_\parallel} = V_A \sqrt{\frac{1+(k_\perp\rho_i)^2}{\beta_i + \frac{2}{1+T_e/T_i}}}}$$

   b. Within ion diffusion region $(k_\perp\rho_i > 1)$, $\frac{\omega}{k_\parallel} \propto (k_\perp\rho_i) V_A$

3. Flux through diffusion region.

a. Now, since $B_{z0} \neq 0$, $\rho_e < \lambda_\perp < \rho_i$

b. Thus, $k_\perp \rho_i \gg 1$ and $k_\perp \rho_e \ll 1$.

c. $n\, U_{out}\, L\delta \sim n(k_\perp \rho_i V_A) L\delta$

d. Now $k_\perp \sim \frac{1}{\lambda_\perp} \sim \frac{1}{\delta}$ (Since $\underset{\sim}{B}_{tot}$ out-of-plane)

e. $n\left(\frac{\rho_i}{\delta} V_A\right) L\delta \sim n_i L \rho_i V_A \leftarrow$ Again, independent of current sheet thickness!

f. Thus, dispersive nature of Kinetic Alfven waves leads to fast reconnection.

4. How big does $b_g = \frac{B_{z0}}{B_{\perp 0}}$ have to be to be in the guide-field regime?

a. Need $\boxed{B_{z0} > 0.1\, B_{\perp 0}}$ such that electron Larmor radius of inflowing electrons with $V_{\perp e} \sim 0.1\, V_{Ae}$ is smaller than d_e, $\rho_e < d_e$

b. Thus, only require $\boxed{b_g > 0.1}$